Simulating the Solar System and Testing the Validity of Kepler's Third Law

Nishwal Gora: s2179934

March 2024

Abstract

By simulating the Solar System using Newtonian dynamics and the Verlet method, it was found that the time step at which the simulation converged was δt, $= 0.5$ days, with the energy fluctuation in the simulation estimated to be 4.36×10^{-3}%. Using this δt, the simulation, conducted over 500 years, demonstrated that the simulated orbital periods, perihelia, and aphelia closely matched theoretical expectations. Additionally, other astronomical phenomena, such as Mercury's apsidal precession, were observed. Furthermore, Kepler's Third Law was validated through the simulation, even when the masses of planets within the Solar System were altered. This also allowed for the investigation of the effect of changing planet sizes on surrounding planets.

Introduction

By simulating an N-body system under the influence of Newtonian gravity, an accurate model of the Solar System can be developed, allowing for precise calculations of observables such as the *perihelia, aphelia* (as well as the perigee and apogee of the Moon) and *orbital periods* of planets. However, these simulations are not exact, with the chosen time step playing a crucial role in determining the accuracy of these observables. This paper aims to establish an accurate model of the Solar System using Python and to test its accuracy against real-world data. It will also examine the fluctuation of the total energy of the system and determine the time step (δt) at which the simulation converges.

Newton's Law of gravitation and gravitational potential

To model the Solar System as an N-body problem, the essential quantities that need to be computed are the separations between planets, the forces exerted among these planets, and the potential energy of the system. Using these calculations, it is possible to model the changes in position of each planet due to the forces exerted by all other planets on it, given initial conditions of mass, position, and velocity. To find the force and potential energy between planet i and j, the following equations were used:

$$\mathbf{F}_{ij} = \frac{G \cdot m_i \cdot m_j}{|\mathbf{r}_i - \mathbf{r}_j|^3} \cdot (\mathbf{r}_i - \mathbf{r}_j) \tag{1}$$

$$V_{ij} = -\frac{G \cdot m_i \cdot m_j}{|\mathbf{r}_i - \mathbf{r}_j|} \tag{2}$$

Where G is the gravitational constant, m_i is the mass of the ith planet, and $\mathbf{r}_i - \mathbf{r}_j$ represents the vector separation between the planets. In an N-body system, it is crucial that the total force on an object is calculated from the $i + 1^{th}$ planet to the n^{th} planet to ensure that the force of a planet on itself, which is undefined, is not calculated. This approach also prevents double counting when calculating the total potential energy of the system.

The Verlet Method

Once the forces, total potential, and positions of the planets are established, it is possible to simulate how the positions and velocities of these planets change over time. For this purpose, the Verlet time integration method can be employed. Utilising the second-order Taylor expansion of $x(t + \delta t)$, and averaging $a(t)$

and $a(t+\delta t)$, provides a more accurate approximation of $v(t+\delta t)$. This enables the determination of position and velocity after a time δt [1].

$$x(t+\delta t) = x(t) + v(t)\delta t + \frac{1}{2}a(t)\delta t^2 \tag{3}$$

$$v(t+\delta t) = v(t) + \frac{1}{2}\left(a(t) + a(t+\delta t)\right)\delta t \tag{4}$$

The simulation proceeds in discrete time steps, δt, and the number of steps for a simulation over time t is given by $\frac{t}{\delta t}$. The Verlet simulation follows a straightforward algorithm:

1) Calculate the initial separations between planets and then the forces (F) on the planets in the Solar System using (1).

2) Update the positions of each planet using (3), acknowledging that $a(t) = \frac{F}{m}$.

3) With these updated positions, new separations and consequently new forces (F_{new}) are calculated, recognising $a(t+\delta t) = \frac{F_{new}}{m}$. Equation (4) is then used to update the velocity, facilitating the calculation of the total kinetic energy at each time step, given by $K = \frac{1}{2}mv^2$.

4) By setting $F = F_{new}$, this process is repeated for the next time step, using the updated values as the new initial conditions.

5) Using $E = K + V$, the total energy of the planetary system is calculated at each time step.

By monitoring the changes in the positions of these planets over time, their orbits can be plotted. Furthermore, by calculating the energy fluctuation:

$$\frac{\Delta E}{E_0} = \frac{E_{Max} - E_{Min}}{E_{initial}} \tag{5}$$

it is possible to test the conservation of energy in the simulation for various δt values.

Elliptical Observables and Kepler's Third Law

An elliptical orbit is characterised by specific observables that define its shape. Foremost among these are the perihelion (r_{per}) and aphelion (r_{ap}), which represent the closest and furthest distances of the orbiting planet from the orbital focus, respectively. In the Solar System, the Sun, around which all other planets orbit, is placed at this focus (F). Assuming this focus as the origin, r_{per} and r_{ap} correspond to the minimum and maximum distances of the planets.

The long axis of the ellipse, known as the "major axis," is given by $r_{per} + r_{ap}$. The semi-major axis, a, is half of this value. Besides these spatial observables, the time a planet takes to complete one rotation around the ellipse is known as the orbital period, T. This period can be determined by the time it takes for a planet to return to its perihelion or aphelion. For nearly circular orbits, the time taken for a planet to complete a rotational angle of 2π can be used.

Identifying these observables is crucial as their convergence serves as another test of the model's accuracy.

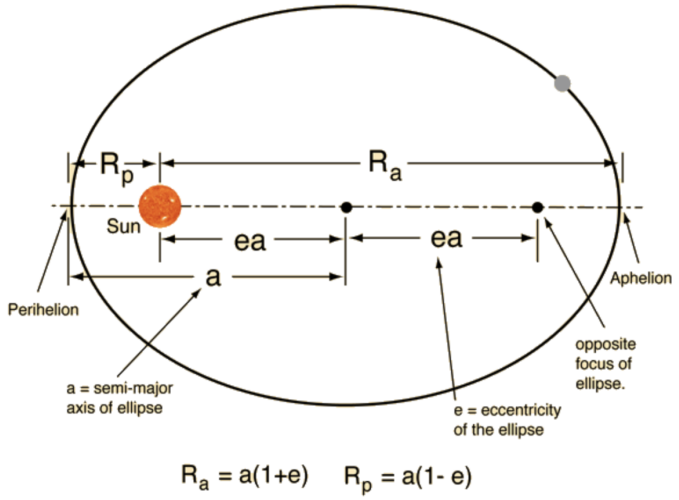

Figure 1: Visual representation of the perihelion, aphelion, major axis, and eccentricity of planets in an elliptical orbit [2]

These observables also facilitate the verification of Kepler's Third Law [3], which posits a proportional relationship between the square of the orbital period (T^2) and the cube of the semi-major axis (a^3):

$$T^2 \propto a^3 \tag{6}$$

Newton's mechanics further refines this relationship by introducing the constant $\frac{(4\pi^2)}{GM}$, where M is the mass of the central body. Consequently, the slope of a plot of T^2 against a^3 depends solely on the mass of the Sun.

The orbits of planets are not perfectly elliptical, with the positions of the apsides (perihelions and aphelions) shifting over time due to various factors, predominantly perturbations from neighbouring planets. Smaller planets are particularly susceptible to these gravitational disturbances [4]. By altering the mass of various planets, the effects of these perturbations can be analysed.

The eccentricity (e) of a planet's orbit quantifies its elliptical nature, defined as:

$$e = 1 - \frac{r_{per}}{a} \tag{7}$$

Here, $e = 0$ indicates a circular orbit, $0 < e < 1$ an elliptical orbit, and $e = 1$ an open parabolic orbit.

Convergence

It was determined that an accurate simulation is one in which the energy fluctuation remains below 0.01%. In simulating a *toy* Solar System consisting of Earth, Earth's Moon, Mercury, and the Sun over 10 years with various δt values, the energy inaccuracy of the simulation was shown to converge when $\delta t =$ 0.5 days, which exhibited an energy inaccuracy of 4.36×10^{-3}%.

A similar convergence was observed in the apsides and orbital period values of Earth and Mercury at δt = 0.5 days. It must be noted, however, that the values of apsides and orbital periods did not precisely match their real-world counterparts, as many planets, moons, and other minor objects were excluded from this *toy* system simulation.

One interesting observation is that only Earth's period did not completely converge after $\delta t = 0.5$ day; in fact, it increased for $\delta t = 0.1$ days, although the overall fluctuation in the apsides decreased beyond

this point.

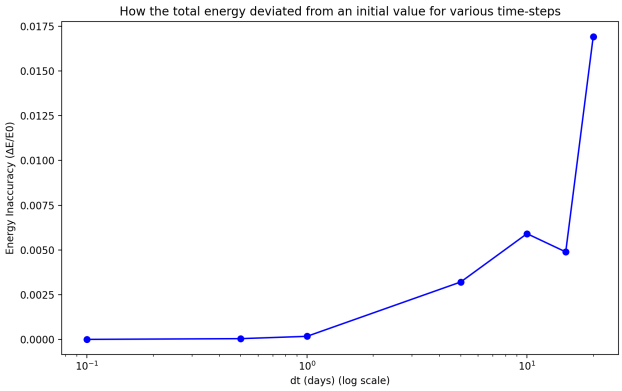

Figure 2: Graph illustrating the negligible change in energy deviation from its initial value beyond $\delta t = 0.5$ days.

Further analysis, simulating every major planet in the solar system, revealed that larger planets farther from the Sun tended to converge at larger δt values than those closer to the Sun. Mercury, however, was an exception, as its particular convergence only occurred at smaller δt values. For instance, when simulated over 100 years at $\delta t = 20$ days, Earth and Venus exhibited orbital periods of 368.78 days and 233.08 days, respectively, whereas Mercury's orbital period significantly diverged from its expected value, showing only 100 days. Similarly, at this δt, Mercury's perihelion and aphelion deviated by almost 0.15 AU from its expected value, while Earth's variance was merely 0.01 AU. Despite Venus, Mercury, and Earth all demonstrating significant deviations from their expected values in the range $20 > \delta t > 10$, Mercury's deviation was of the largest magnitude, as depicted in subsequent figures.

Even more drastic were the fluctuations in the Moon's apogee and orbital period, which ranged from 400 days to 30 days for $20 > \delta t > 1$. Hence, the limiting factors for convergence appear to be particularly the Moon and, more notably, Mercury.

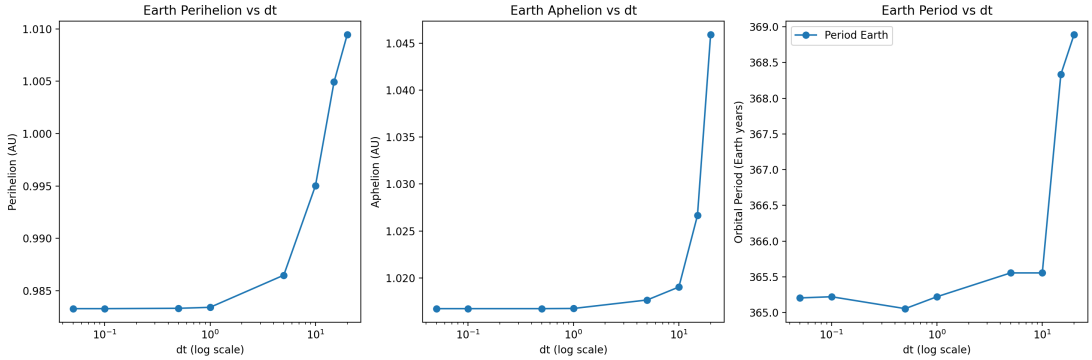

Figure 3: Plot illustrating the convergence of Earth's apsides and orbital period at $\delta t = 0.5$ days.

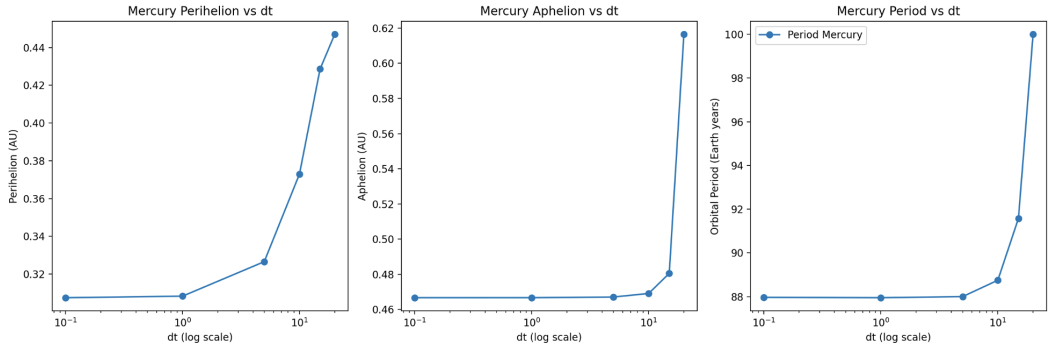

Figure 4: Plot illustrating the convergence of Mercury's apsides and orbital period at $\delta t = 0.5$ days.

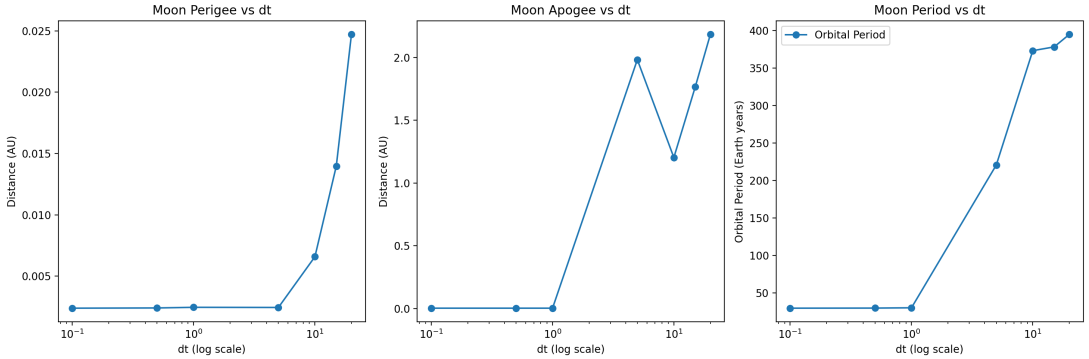

Figure 5: Plot illustrating the convergence of the Moon's apsides and orbital period at $\delta t = 0.5$ days.

From this analysis, a $\delta t = 0.5$ days has been adopted as a suitably accurate interval for simulating future results.

Results

Using this value of δt, a more realistic (yet incomplete) solar system was simulated. The results of various observables of orbiting objects, simulated over 500 years are shown below.

Table 1: Comparison of Simulated and Observed Orbital Observables [5]

Orbiting Body	**Orbital Period (Days)**		**Perihelion (AU)**		**Aphelion (AU)**	
	Simulated	Theoretical	Simulated	Theoretical	Simulated	Theoretical
Mercury	87.968	87.97	0.30768	0.3075	0.46671	0.467
Venus	224.715	224.7	0.71843	0.7184	0.72830	0.7282
Earth	365.268	365.25	0.98327	0.9833	1.01674	1.0167
Moon[1]	29.663	27.32	0.0024	0.00257	0.0027	0.00270
Mars	686.992	687	1.38050	1.3814	1.66679	1.666
Jupiter	4332.451	4332	4.94195	4.950	5.46238	5.454
Saturn	10767.375	10759	9.00848	9.041	10.0798	10.123
Uranus	30715.8	30685	18.2540	18.286	20.1215	20.098
Neptune	60197	60182	29.7981	29.809	30.3579	30.33
Pluto	90602.5	90560	29.6452	29.658	49.3505	49.305
1P/Halley	27018.42	27120-28855	0.59016	0.586	35.1434	35.14

Apsides and Orbital Periods

It is evident that, despite neglecting minor moons and other orbiting objects in the Solar System, the simulation provides an accurate model when compared to observed results. Furthermore, the difference between simulated and actual observed/theoretical results indicates an increase in the fractional error of the orbital period as expressed by the following equation:

$$\frac{\Delta x}{x_{obs}} = \frac{x_{obs} - x_{sim}}{x_{obs}} \tag{8}$$

This trend suggests that planets with shorter orbital periods (T), completing a greater number of orbits, yield more accurate T_{sim} values. This accuracy arises because the Standard Error on the Mean (SEM) decreases as $1/\sqrt{N}$. Beyond the orbital periods, the apsides demonstrated a similar pattern. For instance, the fractional error on Mercury's perihelion (r_{per}) was 5.85×10^{-4}, while that of Uranus was 1.75×10^{-3}. However, there isn't a consistent upward trend, as evidenced by Saturn's fractional error on r_{per} being greater than that of Uranus. This variation occurs because the algorithm employed for these calculations was based on a continuously updated list capturing the furthest distance from the Sun, rather than an average.

The plot of Earth's orbit around the Sun confirms a stable orbit with aphelion and perihelion distances approximately 1 AU, aligning with expectations. This pattern was consistent across other planets, with the exception of Mercury. Throughout the simulation, Mercury's perihelion and aphelion distances varied, indicating significant apsidal precession.

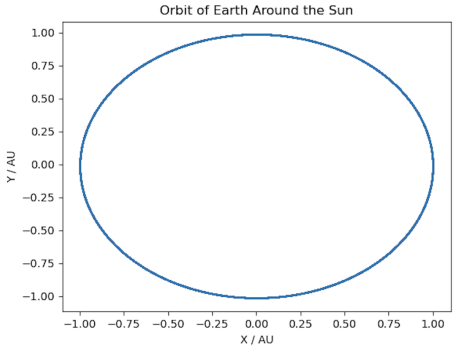

Figure 6: Figure illustrating that over 500 years, Earth's r_{ap} and r_{per} distances remained consistent.

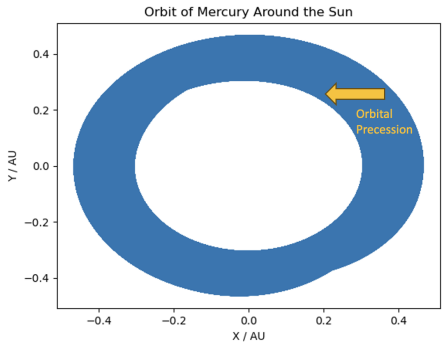

Figure 7: Figure showing Mercury's apsidal precession throughout the 500-year simulation.

Given that the simulation utilised Newtonian Mechanics, the primary factor influencing Mercury's apsidal precession is the gravitational perturbations from surrounding planets such as the Earth and Venus [6], and its proximity to the Sun.
Apart from Mercury, 1P/Halley exhibited a distinctly different orbit from the other planets. Not only did it demonstrate a greater level of apsidal precession, but its orbit also showed a significant tilt compared to others. This variance is primarily due to its greater inclination to the ecliptic plane, alongside an eccentricity of 0.967 obtained from the simulation, which positions its orbit close to parabolic rather than elliptical. This is in stark contrast to the orbits of planets like Jupiter and Saturn, whose eccentricities were recorded at 0.050 and 0.056, respectively.

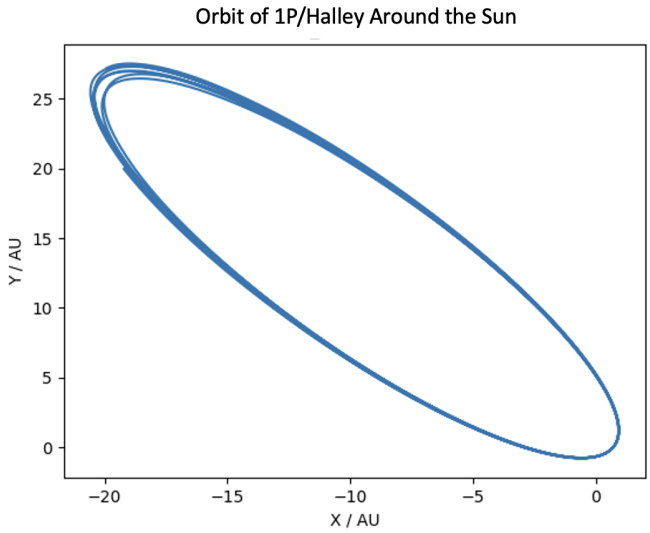

Figure 8: Figure depicting a tilted and precessed orbit of 1P/Halley.

Orbiting Body	Eccentricity
Mercury	0.2054
Venus	0.0068
Earth	0.0167
Mars	0.0939
Jupiter	0.0500
Saturn	0.0561
Uranus	0.0487
Neptune	0.0093
Pluto	0.2494
Halley's Comet	0.9670

Figure 9: Eccentricities of Planets and Halley's Comet.

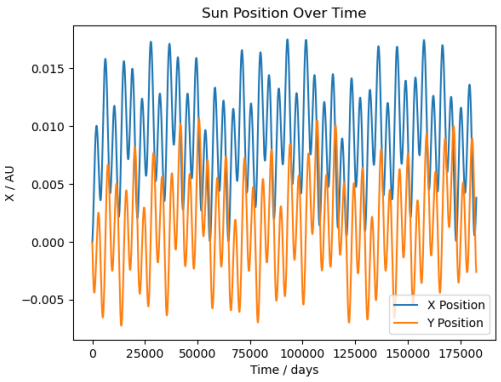

Figure 10: Figure demonstrating the negligible shift in the Sun's position over time.

Moreover, the stability of the Sun's position throughout the simulation was analysed. Despite minor perturbations attributed to the gravitational influences of planets and potential inaccuracies inherent in the Verlet simulation method, these deviations remained below 0.02 AU, thus considered negligible to the overall precision of the simulation, especially as the planetary positions were calculated relative to the Sun at each moment.

Verifying Kepler's Third Law

The 500-year simulation with $\delta t = 0.5$ days verified Kepler's Third Law, demonstrating a linear relationship between T^2 and a^3 as anticipated.

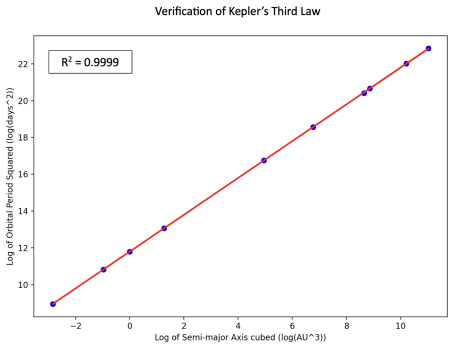

Figure 11: Illustration of Kepler's law within the simulation of the planets orbiting the Sun.

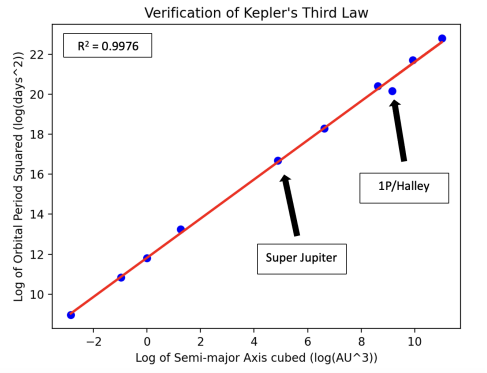

Figure 12: Effects on Kepler's law by increasing Jupiter's mass by a factor of 20.

Theoretically, the slope of the plot should remain unchanged regardless of the mass of the orbiting bodies. However, in simulations excluding *super Jupiter*, the slope was found to be 0.9993 s^2/m^{-3}. Introducing super Jupiter (Jupiter with its mass scaled up by 20) slightly altered the slope to 0.9790 s^2/m^{-3}. Despite this, both plots maintained $R^2 > 0.99$, confirming T^2's linear proportionality to a^3, even with super Jupiter's inclusion. Nonetheless, inherent inaccuracies in the simulation caused a change in the slope, which theoretically should remain constant.

Planet	$\frac{\Delta T}{T}$	$\frac{\Delta r_{per}}{r_{per}}$	$\frac{\Delta r_{ap}}{r_{ap}}$
Mercury	0.0080	0.0004	0.0003
Venus	0.0003	0	0
Earth	0.0007	0.0005	0.0001
Mars	0.0912	0.0054	0.0035
Jupiter	0.0359	0.0002	0.0364
Saturn	0.1336	0.1010	0.0025
Uranus	0.125	0.1551	0.0106
Neptune	0.1400	0.1682	0.0126
Pluto	0.0155	0.052	0.02453
1P/Halley	0.1180	0.0115	0.1784

Table 2: Fractional Shift in Orbital Characteristics with Super Jupiter.

Although both systems display high R^2 values, the presence of *super* Jupiter led to a less robust correlation (Lower R^2 value) , particularly for planets like Saturn, Uranus, and Neptune. Their proximity to Jupiter resulted in greater shifts in their T, r_{per}, and r_{ap} compared to inner planets. The instability introduced by super Jupiter was most evident in the apsidal precession observed in Saturn's orbit and significantly in 1P/Halley's orbit.

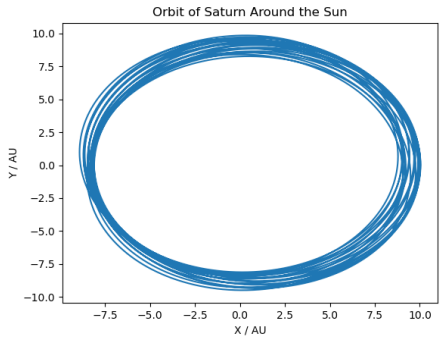

Figure 13: Minor precession in Saturn's orbit following the introduction of Super Jupiter.

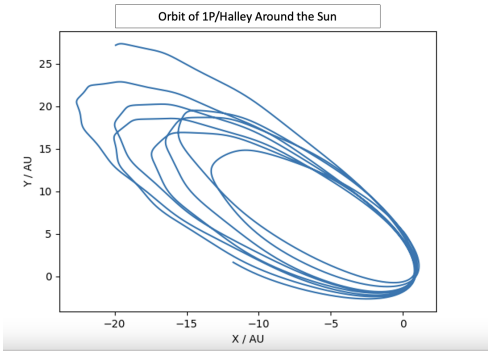

Figure 14: Significant influence of Super Jupiter on 1P/Halley's orbit, leading to more unstable variations in its apsides.

1P/Halley's eccentricity increased to 0.972, making its orbit nearly parabolic and further from being elliptical compared to a standard Solar System setup. Notably, despite significant shifts in the observables of Neptune and Uranus, their precession was minimal. Furthermore, the orbits of planets closer to the Sun remained largely unaffected by Jupiter's mass increase, due to the dominant gravitational influence of the Sun on these inner planets.

Conclusion

Within the bounds of experimental error, this simulation of the Solar System was shown to align with physical predictions, accurately determining the orbital periods, perihelia, and aphelia of celestial bodies. It was found that the energy deviation converged at a time step of $\delta t = 0.5$ days, thereby setting this interval as the standard for future simulations to ensure accuracy. Moreover, while most planets exhibited stable orbits with minimal apsidal precession, Mercury and 1P/Halley displayed significant apsidal precession due to their relatively low masses.

Additionally, the Sun's movement was found to be negligible, allowing it to be considered stationary at the centre of the Solar System. This simplification can facilitate future simulations by negating the need to account for its positional changes.

The eccentricity values obtained for the planetary bodies corroborated their expected orbital shapes, with 1P/Halley approaching a nearly parabolic orbit and Neptune demonstrating an almost circular trajectory, as anticipated. Kepler's Third Law was also validated within this simulated system, even when Jupiter's mass was increased twentyfold. However, this alteration in mass notably affected the orbits of neighbouring planets, while having minimal impact on those more distant or closer to more massive bodies, such as the Sun.

Overall, the simulation proved to be accurate when simulated at δt= 0.5 days. Hence only minor changes can be made to it, mainly to increase its efficiency and allow it to be run for smaller δt values. Secondly, though only Neptune's perihelion and aphelion were found by specifying its orbit to be nearly circular, further study has shown that the orbit of Venus is similarly circular. Hence, the function used for Neptune can be utilised for Venus.

Further, the simulation is specifically made to accommodate specific input files in which the planets (specifically the Earth, Moon, Sun and Neptune) are all spelt in a specific way. Future work can be built on ensuring the scope of the simulation is not hindered in this way.

References

1. Verlet, L. Computer experiments on classical fluids. I. Thermodynamical properties of Lennard-Jones molecules. *Physical review* **159,** 98 (1967).
2. *Kepler's Laws* `http://hyperphysics.phy-astr.gsu.edu/hbase/kepler.html`. 12th March, 2024.
3. Haubold, H. J. in *Encyclopedia of Planetary Science* 379–380 (Springer Netherlands, Dordrecht, 1997). ISBN: 978-1-4020-4520-2. `https://doi.org/10.1007/1-4020-4520-4_208`.
4. Kipping, D. M. *The transits of extrasolar planets with moons* (Springer Science & Business Media, 2011).
5. Williams, D. D. R. *Planetary Fact Sheet - Metric* `https://nssdc.gsfc.nasa.gov/planetary/factsheet/`. Accessed: your access date here. NASA Goddard Space Flight Center, 2024.
6. Park, R. S. *et al.* Precession of Mercury's Perihelion from Ranging to the MESSENGER Spacecraft. *The Astronomical Journal* **153,** 121 (2017).

Appendix

Plots from Simulation

Here, the orbital plots of planets in the simulation are reproduced, showing visually the perihelion and aphelion values obtained in Table 1.

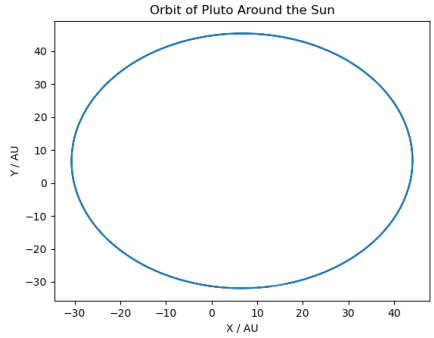

Figure 15: Orbit of Pluto

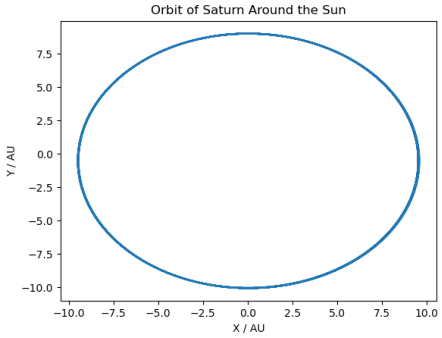

Figure 16: Orbit of Saturn

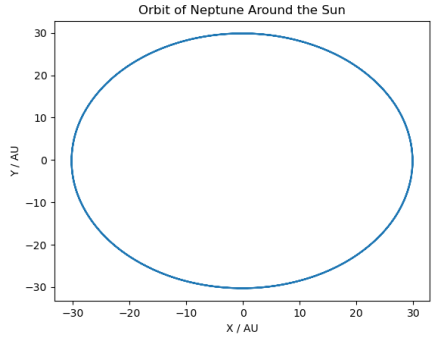

Figure 17: Orbit of Neptune

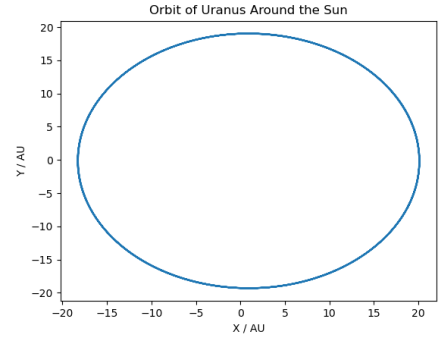

Figure 18: Orbit of Uranus

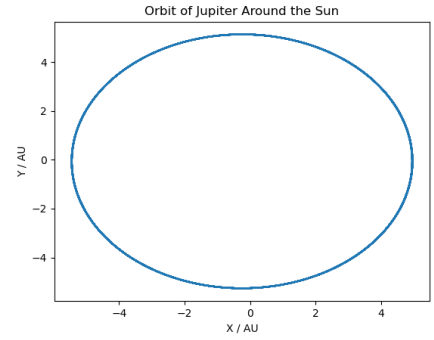

Figure 19: Orbit of Jupiter

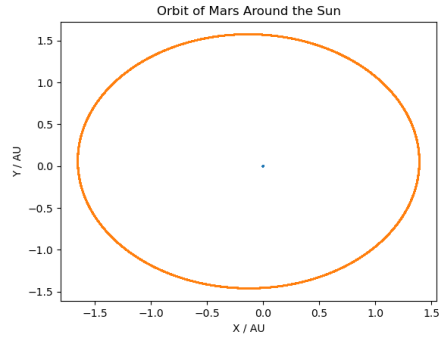

Figure 20: Orbit of Mars